Screening and Characterization of Glucuronoyl Esterase Candidates from the CE15 Family

Junyang Wang

Biotechnology, LTH

Supervisor: Savvina Leontakianakou

Examinaer: Eva Nordberg Karlsson

LUND UNIVERSITY

LTH

FACULTY OF ENGINEERING

Abstract

This study aimed to screen and characterize unknown glucuronoyl esterases (GEs) belonging to bacterial carbohydrate esterase family 15 (CE15), which were CE15_6nl, CE15_13nl, and CE15_15nsp. First, purified proteins were obtained by heterologous expression in *E. coli* induced by IPTG. Next, nanoDSF assays were performed to determine the thermostability of CE15 enzymes under different pH conditions, CE15_6nl and CE15_15nsp were most stable under pH 7 and pH 6.5, respectively, whereas CE15_13nl was more stable under alkaline conditions. Moreover, kinetics parameters were determined by coupled continuous assays on three model substrates. CE15_15nsp exhibited the highest catalytic efficiency and substrate affinity among the three enzymes. All candidates showed a preference for long substrates. To explore the action of single CE15 enzyme and CE15-GH30 synergy in the hydrolysis of natural biomass such as corn bran, HPAEC-PAD analysis was conducted. The results suggested that CE15 enzymes promoted the release of xylose and xylo-oligosaccharides, however, no synergistic effect between CE15 and GH30 could be detected. In total, CE15 enzymes show promising potential in lignocellulosic biomass processing, but further analytical experiments are required.

Popular Scientific Abstract

Fossil fuels are a major driver of climate change and environmental pollution, causing substantial impacts on ecosystems and human health. Lignocellulosic biomass is a promising alternative to fossil fuel. However, the treatment of lignocellulosic biomass remains challenging for industrial application partially due to the recalcitrance of lignin-carbohydrate complexes (LCCs). Since 2006, glucuronoyl esterase (GEs) from carbohydrate esterase family 15 (CE15) have been discovered, and it has been shown that they were able to hydrolyze ester bonds between lignin and carbohydrates. Compared with fungal GEs, bacterial GEs have been reported to show wider substrate specificity, but many bacterial GEs remain uncharacterized.

Therefore, this study focused on screening and characterizing unknown bacterial GEs. Three bacterial GEs were obtained and characterized. Their stability under different conditions was determined. Two of them were most stable under neutral or slightly acidic conditions, while another CE15 enzyme showed higher stability under alkaline conditions. Moreover, these enzymes showed GE activity on different substrates even on natural biomass. Bacterial GEs have the potential to assist in the degradation of lignocellulosic biomass.

Table of Content

Abstract ..... *i*
Popular Scientific Abstract ..... *ii*
1. Introduction *1*
1.1 Lignocellulosic biomass **1**
1.1.1 Cellulose 2
1.1.2 Hemicellulose 2
1.1.3 Lignin 3
1.2 Lignin-carbohydrate complexes (LCCs) in plant cell walls **4**
1.3 Carbohydrate-active enzymes **6**
1.3.1 Glucuronoyl esterases (GEs) 6
1.3.2 Glycoside hydrolase family 30 (GH30) 7
1.4 Aim of the study **8**
2 Materials and Methods *9*
2.1 Materials **9**
2.1.1 Plasmids and Strains 9
2.1.2 Chemical Reagents 9
2.2 Methods **10**
2.2.1 Screening and obtaining glucuronoyl esterases from bacteria 10
2.2.2 Analysis of biochemical characterization of purified proteins 13
2.2.3 Enzymatic activity and kinetic analysis on model substrates 14
2.2.4 Enzymatic activity on complex substrate 14
3 Results *15*
3.1 Determination of protein thermal stability **15**
3.2 Verification of glucuronoyl esterase activity **15**
3.3 Storage stability **16**
3.4 Biochemical characterization and substrate specificity of CE15 enzymes **17**
3.5 Analysis of enzymatic activity on pretreated corn bran **18**
3.5.1 Hydrolysis action pretreated corn bran by individual CE15 enzymes 18
3.5.2 Synergetic effect of GEs and GH30 on pretreated corn bran 19
4 Discussion *20*
5 Conclusion *21*
6 Acknowledgment *22*
7 References *23*
8 Appendix *29*

1. Introduction

1.1 Lignocellulosic biomass

As global concerns over fossil fuel depletion and environmental degradation continue to grow, biomass has emerged as one of the most promising renewable alternatives, offering significant potential to produce bioenergy and biomaterials while introducing far fewer harmful effects on ecosystems and human health (Ragauskas et al., 2006). Among the various biomass feedstocks, lignocellulosic biomass is particularly noteworthy, around 181.5 billion tons of lignocellulosic biomass is generated per year that needs to be deconstructed into its monomers (Paul & Dutta, 2018), which can be found in both forest and agricultural systems. Lignocellulosic biomass is considered as next-generation feedstocks since it has no competition with any food crops and arable lands (Nanda et al., 2018). A wide variety of lignocellulosic biomass, including rice, wheat, barley straw, and sugarcane bagasse, have been utilized in bioenergy production (Shah et al., 2022). Lignocellulosic biomass "plant cell wall" is the largest reservoir of polysaccharides on earth (Bauer et al., 2006), which is composed of three major natural polymers: cellulose, hemicelluloses, and lignin, forming a recalcitrant network (**Figure 1-1**). These polymers can be converted into biofuels, green polymers, and other bio-based materials (Gandini, 2011; Ragauskas et al., 2006). Bioenergy production relies primarily on the conversion of cellulose and hemicellulose to their monomeric compounds (Brethauer & Wyman, 2010). However, the natural recalcitrance of lignocellulosic biomass limits enzymatic and biochemical degradation, due to the crystallinity of cellulose, the hydrophobicity of lignin, and the encapsulation of cellulose within the lignin-hemicellulose matrix (Agbor et al., 2011; Barakat et al., 2013). Therefore, the effective utilization of lignocellulosic biomass is widely regarded as a critical strategy for reducing reliance on fossil resources and advancing global goals of energy security, environmental sustainability, and socioeconomic development.

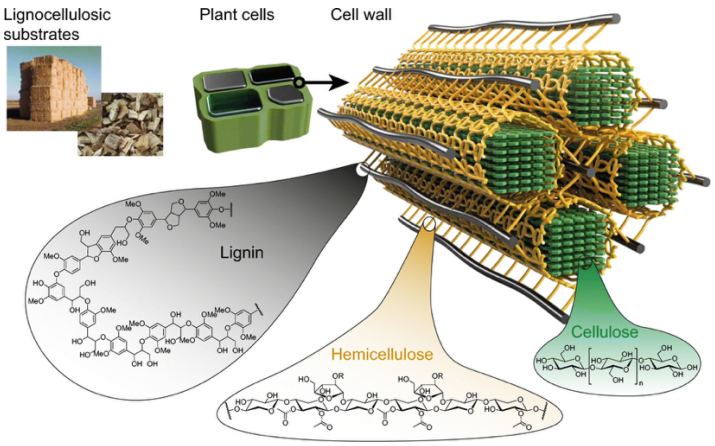

Figure 1-1. The complicated structure of plant cell wall, mainly composed of cellulose, hemicellulose, and lignin (Brethauer et al., 2020).

1.1.1 Cellulose

Cellulose is a linear, fibrous polysaccharide composed of long chains of 7000-15,000 D-glucose units that are linked through *β*-1,4-glycosidic bonds (**Figure 1-2**), in which the C1 anomeric carbon of one glucose unit is linked to the C4 hydroxyl group of the adjacent glucose unit (Gibson, 2012). The high degree of polymerization of cellulose, ranging from 300-5000, contributes to its resistance to degradation (Aulin et al., 2009). Cellulose molecules associate through extensive hydrogen bonding to form tightly packed bundles known as cellulose microfibrils (Aulin et al., 2009). As a major structural component of plant cell walls, cellulose microfibrils provide mechanical strength and contribute to the rigidity and stability of the cell wall. In addition, six polymorphs of cellulose were uncovered that are cellulose I, II, III_1, III_{11}, IV_1, and IV_{11}. Cellulose I is the form existing in nature, and other forms were formed by processing cellulose I such as regeneration, mercerization, and heating (O'Sullivan, 1997).

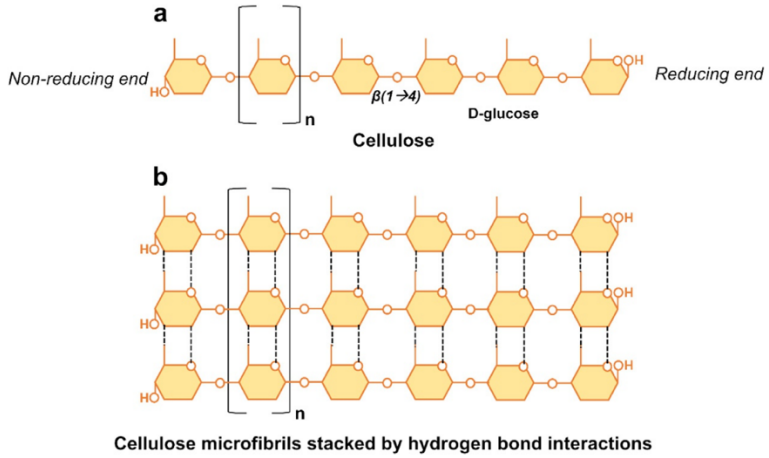

Figure 1-2. Structure of cellulose and cellulose microfibrils (Gavande et al., 2023). (a) Cellulose is a linear polysaccharide composed of β-D-glucose units linked by β-1,4-glycosidic bonds. Each chain has a non-reducing end and a reducing end. (b) Cellulose chains are assembled into microfibrils through extensive hydrogen bond interactions.

1.1.2 Hemicellulose

Hemicellulose is another major structural polysaccharide fraction in lignocellulosic biomass, the content of hemicellulose is highly dependent on the plant species, accounting for approximately 10–25% (Wang et al., 2017). In contrast to cellulose, hemicellulose is not a single polymer but a heterogeneous group of branched polysaccharides with relatively low degrees of polymerization, usually around 50–200 (Chen, 2014a). It is composed of various sugar residues, including pentoses, hexoses, and uronic acids (**Figure 1-3**), which form polymers such as xylans, mannans, glucomannans, galactomannans, and xyloglucans. Moreover, the composition of hemicellulose varies among plant species.

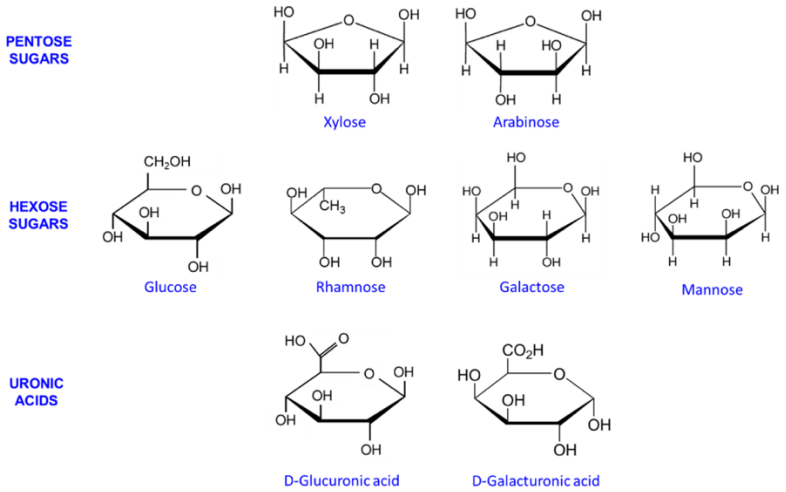

Figure 1-3. Structures of different hemicellulose sugars and uronic acids (Okolie et al., 2021).

Xylans usually have a *β*-1,4-linked D-xylose backbone with different decorations, such as arabinose, D-glucuronic acid, ferulic acid, and acetyl groups. Mannans are based mainly on β-1,4-linked mannose residues and include glucomannans and galactomannans. Because of these different backbone structures and substitutions, hemicellulose is more heterogeneous than cellulose and requires multiple enzymes for degradation (Yeoman et al., 2010).

1.1.3 Lignin

Lignin is a complex aromatic polymer mainly biosynthesized from three monolignol precursors: *p*-coumaryl alcohol, coniferyl alcohol, and sinapyl alcohol (Pandey & Kim, 2011). During lignification, these monolignols are incorporated into the lignin polymer and generate the corresponding *p*-hydroxyphenyl (H), guaiacyl (G), and syringyl (S) units, respectively (Chen, 2014b; Okolie et al., 2021) (**Figure 1-4**). These units are randomly connected through different linkages, resulting in a highly heterogeneous and recalcitrant lignin structure. In lignocellulosic biomass, lignin surrounds and interacts with cellulose and hemicellulose, forming a dense matrix that limits enzyme accessibility to polysaccharides, especially for hemicellulose. Lignin can be covalently associated with hemicellulose through lignin–carbohydrate linkages, which further increases the resistance of plant cell walls to degradation and protects cellulose (Lawoko et al., 2005). Therefore, reducing or disrupting the lignin barrier is an important step to improve the exposure of cellulose microfibrils and hemicellulose, thereby facilitating enzymatic hydrolysis and subsequent microbial fermentation into alcohols (Nanda et al., 2014).

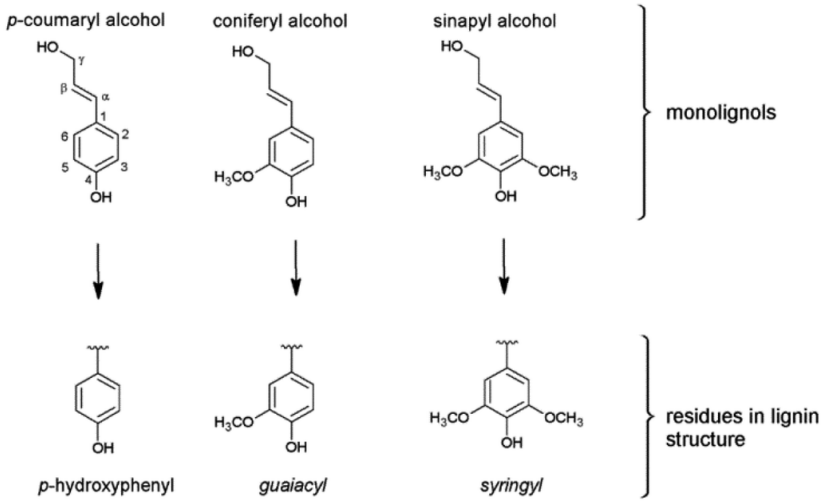

Figure 1-4. Three chemical structures of monolignol precursors in lignin and structural units (Okolie et al., 2021).

1.2 Lignin-carbohydrate complexes (LCCs) in plant cell walls

The plant cell walls are composed of middle lamella, primary cell wall (PCW), and secondary cell wall (SCW). In general, to avoid attack from microorganisms, most of the mass and energy content is found in SCWs, in which lignin and carbohydrate moieties are chemically cross-linked, forming lignin-carbohydrate complexes (LCCs) (Himmel et al., 2007; Singhvi & Gokhale, 2019). LCCs is a significant contributor to the recalcitrance since it serves as the intermolecular connection bridge between the lignin and polysaccharides (Agger et al., 2023). Moreover, several studies have shown that LCCs can hinder biomass conversion by affecting the efficiency of enzymatic hydrolysis and reducing cellulose accessibility for enzymatic reactions (Balan et al., 2009; Laureano-Perez et al., 2005).

Different types of lignin-carbohydrate linkages have been identified in both softwoods and hardwoods. These linkages are generated during lignin biosynthesis through oxidative coupling reactions (Eriksson et al., 1980; Jin et al., 2006; Lam & Iiyama, 2000; Santos et al., 2013). At present, major LCC linkages are determined, including benzyl ether, benzyl ester, ferulate ester, phenyl glycosidic, and diferulate esters (**Figure 1-5**). Benzyl ester bonds are formed between the carboxyl groups of carbohydrate-derived uronic acids and hydroxyl groups on lignin side chains. Benzyl ether and phenyl glycosidic linkages connect carbohydrate residues, such as glycosyl or mannosyl units, with benzylic or phenolic hydroxyl groups in lignin (Wegener, 2004).

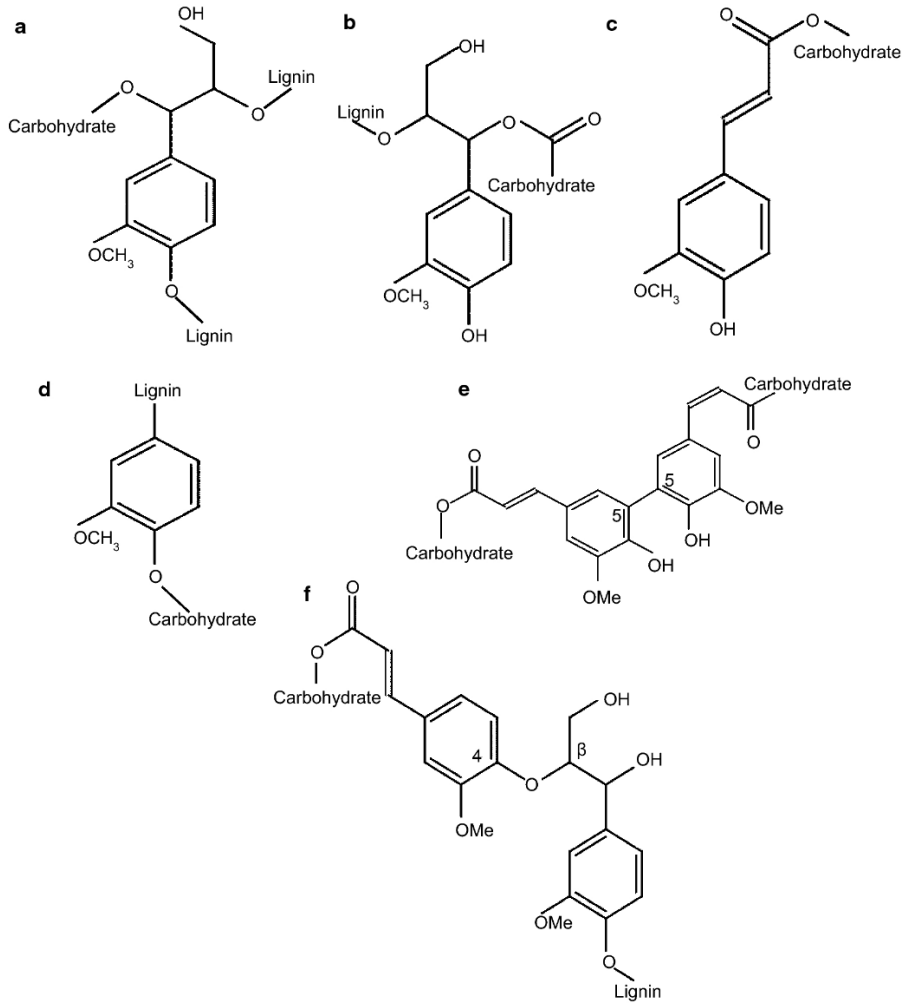

Figure 1-5. LCC linkages (Main types of LCC linkages: **a** benzyl ether; **b** benzyl ester; **c** ferulate ester; **d** phenyl glycosidic; **e** diferulate ester (5′–5′ linkage); **f** diferulate ester (4-O-*β* linkage) (Tarasov et al., 2018).

The ester-linked LCC exists between the carboxylic moiety of 4-O-methyl-D-glucuronoyl substitutions on glucuronoxylan and the *γ*-positioned or *α*-positioned hydroxyls on lignin (Balakshin et al., 2011; Sapouna & Lawoko, 2021) (**Figure 1-6**). To date, only this ester bond can be hydrolyzed directly by enzymatic cleavage.

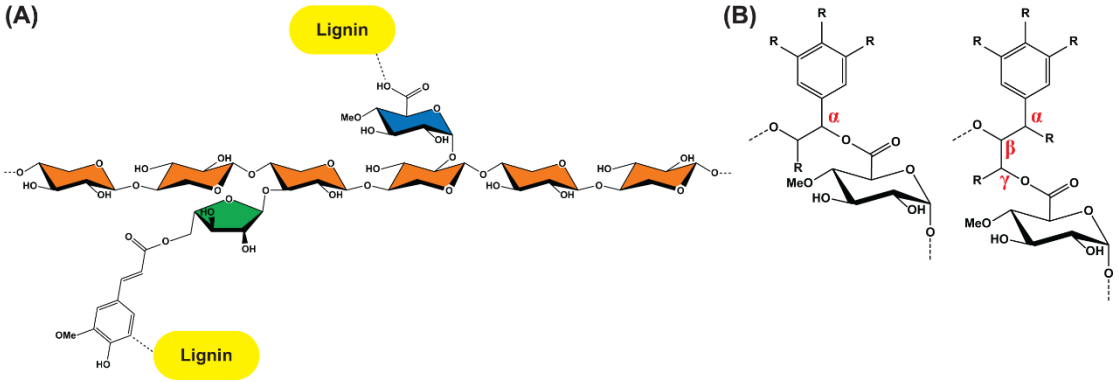

Figure 1-6. (A) Lignin covalently binds to glucuronoxylan through ester linkages to 4-O-methyl-D-

glucuronoyl moieties or feruloylated side chains. (B) Two configurations of ester linkages between 4-O-methyl-D-glucuronoyl and lignin in α-positioned or γ-positioned. (Larsbrink & Lo Leggio, 2023)

1.3 Carbohydrate-active enzymes

Complex carbohydrates are widely distributed in nature and occur in various forms, including polysaccharides, glycolipids, and glycoproteins, which are vital energy sources for all forms of life. Monosaccharides can be linked through different glycosidic linkages to form diverse polysaccharides, such as cellulose, hemicellulose, and lignin (Laine, 1994). In nature, carbohydrates are mostly present as stable polymeric or conjugated structures, and their degradation into monomeric forms is essential for sustaining the carbon cycle, which generally requires enzymatic deconstruction into smaller oligosaccharides or monosaccharides (Gavande et al., 2023). Carbohydrate-active enzymes (CAZymes) play essential roles in both the biosynthesis and degradation of carbohydrates, acting on a wide range of substrates with diverse catalytic specificities (Henrissat, 1991; Henrissat et al., 1989; Henrissat & Bairoch, 1993). CAZymes are classified into several major classes based on their amino acid sequence similarities and catalytic mechanisms, including glycoside hydrolases (GHs), glycosyltransferases (GTs), polysaccharide lyases (PLs), carbohydrate esterases (CEs), auxiliary activity enzymes (AAs), and carbohydrate-binding modules (CBMs). The CAZy database (http://www.cazy.org), established in 1998, currently encompasses hundreds of protein families across these classes.

1.3.1 Glucuronoyl esterases (GEs)

The first GE was discovered in the fungus *Schizophyllum commune* in 2006, when it was shown that GEs were able to hydrolyze methyl ester of 4-O-methyl-D-Glcuronic acid (4-O-D-GlcA), (Špániková & Biely, 2006). The homologous Cip2 from *Trichoderma reesei* was also determined to possess the GE activity, allowing a new carbohydrate esterase family 15 (CE15) to be established (Li et al., 2007). Researchers started to pay attention to GEs from microorganisms.

Initially, GEs activity was determined by using synthetic model substrates (Me)GlcA-based esters such as benzyl D-glucuronate. Generally, the preference towards bulkier substrates was discovered by comparing the kinetic parameters of different substrates (d'Errico et al., 2015). GEs also cleaved ester bonds on more complex substrates. AaGE1 from *Acremonium alcalophilum* treatment was observed to degrade the LC ester linkages existing in spruce- and birch woods (Arnling Bååth et al., 2016a). To utilize the plant cell wall polymers as a nutrient source, biomass-degrading microorganisms (both bacteria and fungi) are required to produce multiple secreted enzymes to overcome this robust matrix (Rosso et al., 2022). De Santi et al. classified CE15 sequences into two major clades, B (Bacteria) and F (Fungi), according to their taxonomic origins. Clade B consists exclusively of bacterial sequences, whereas clade F is dominated by fungal members but also includes a small subset of bacterial sequences (De Santi et al., 2016). The catalytic domain sequences of bacterial CE15 enzymes are more diverse than those of fungal GEs. Even within a single species, multiple CE15 enzymes can be encoded, as seen in *Opitutus terrae*, where *Ot*CE15A, B, C, and D are distributed across the phylogenetic tree and differ in catalytic efficiency and substrate specificity (Arnling Bååth et al., 2018a). In

contrast, the catalytic domains of fungal GEs are more clustered (Larsbrink & Lo Leggio, 2023).

1.3.1.1 Fungal GEs

Research about GEs began shedding light since the first GE was found from the fungus *S. commune* (Špániková & Biely, 2006). Beyond their native activity, fungal GEs have been shown to prefer substrates with 4-O-methylation, and they exhibited less or no activity on substrate without this substitution, indicating the importance of 4-O-methylation for fungal GEs (Arnling Bååth et al., 2016b; d'Errico et al., 2015; Špániková et al., 2007). As stated in the introduction above in **1.3.1**, fungal GEs also prefer to degrade larger substrates, supporting the proposed biological function of GEs on LCCs (d'Errico et al., 2015). Substrate specificity was examined on several substrates, including galacturonate esters, feruloyl- and acetyl esters. Fungal GEs only showed activity on glucuronate esters, with no detectable activity on others (Ďuranová et al., 2009; Špániková et al., 2007; Špániková & Biely, 2006).

1.3.1.2 Bacterial GEs

Both bacterial and fungal GEs share a preference for bulkier substrates. However, unlike fungal GEs, bacterial GEs are not sensitive to methylation on glucuronic acid. Interestingly, several GEs showed little or no difference in activity among different alcohol moieties, and a few GEs exhibited notable differences toward benzyl, allyl, and methyl glucuronates. Moreover, bacterial GEs showed comparative k_{cat}/K_m (s^{-1} M^{-1}) values on galacturonate esters, indicating that a broader substrate specificity compared to fungal GEs (Arnling Bååth et al., 2018b). In addition, they strongly increased the release of monosaccharides in hydrolysis of corn cobs when supplemented in the enzyme cocktail, suggesting an essential role of CE15 enzymes in promoting more efficient enzymatic reactions for processing natural biomass (Arnling Bååth et al., 2018b). Bacterial GEs are proposed to act on ester bonds at the initial stage of plant cell wall degradation (Larsbrink & Lo Leggio, 2023), as for example *Tt*CE15A is competitively inhibited by xylooligosaccharides and aromatic compounds (Arnling Bååth et al., 2019), yet it retains the capacity to release sugars from LCCs without being hindered by the main chain xylan polysaccharides (Raji et al., 2021).

1.3.2 Glycoside hydrolase family 30 (GH30)

Glycoside hydrolase (GH) is a major category within the CAZymes and are responsible for the hydrolysis of the glycosidic linkages in polysaccharides (Gavande et al., 2023), and promotion of transglycosylation reactions. GH is classified as EC 3.2.1 group of Enzyme Commission, which distributes in 173 different families annotated as GH1 to GH173 In addition, the function of GH30 possesses wide diversity, including β-glucosidases (3.2.1.21), β-glucuronosidases (EC 3.2.1.31), β-xylosidases (3.2.1.37), β-fucosidases (EC 3.2.1.38), glucosylceramidases (EC 3.2.1.45), β-1,6glucanases (EC 3.2.1.75), glucuronoarabinoxylan endo-β1,4-xylanase (EC 3.2.1.136), and endo-β-1,6-galactanase (EC 3.2.1.164). The GH30 family comprises 8 subfamilies, and enzymes belonging to bacterial GH30_8 have been characterized as appendage-dependent, as they act on xylan decorated with 4-O-methyl-D-glucuronic acid (MeGlcA) side substituents (Biely et al., 2014; St John et al., 2010). These enzymes showed no or slower activity when they act on glucurnoxylan without MeGlcA (St. John et al., 2006; Vršanská et al., 2007).

1.4 Aim of the study

The purpose of this study was to screen and characterize novel bacterial GEs. Candidate GEs were produced by heterologous expression and purified for biochemical characterization, including thermostability analysis and determination of kinetic parameters toward model substrate. Furthermore, the ability of GEs to act on a natural complex substrate was evaluated by HPAEC-PAD, both exclusively with CE15 and in sequential incubation with GH30.

2 Materials and Methods

2.1 Materials

2.1.1 Plasmids and Strains

All strains and plasmids used in this study were shown in **Table 2-1**.

Table 2-1. ***Competent cells and plasmids used in this study.***

Plasmid	Competent cell (*E. coli*)	
pET21b (+)-CE15_6nl	Tuner(DE3)	Used in biochemical characterization
pET21b (+)-CE15_13nl	Rosetta2(DE3)	
pET21b (+)-CE15_15nsp	BL21(DE3)	
pET21b (+)-CE15_2nl	Tuner(DE3) BL21(DE3)	
pET21b (+)-CE15_2nsp	Rosetta2(DE3) BL21(DE3)	
pET21b (+)-CE15_6nsp	BL21(DE3) Tuner(DE3)	
pET21b (+)-CE15_7nsp	BL21(DE3) Tuner(DE3)	
pET21b (+)-CE15_7nl	BL21(DE3) Rosetta2(DE3)	
pET21b (+)-CE15_9nl	Tuner(DE3)	
pET21b (+)-CE15_13nl	Rosetta2(DE3)	

2.1.2 Chemical Reagents

LB medium (The Difco Lennox Broth was purchased from BD), Mcllvaine pH buffer, Dimethyl Sulfoxide (DMSO), BOXyn30A (GH30_8 was purchased from NZYtech), PBS, 1M IPTG, 100mg/L Ampicillin, HEPES binding buffer, HEPES elution buffer, K-URONIC Kit

(Megazyme, Ireland), corn bran, NaOH, NaOAc, MilliQ-Water.

Model substrates used in the kinetics assay: Benzyl D-glucuronate (BnzGlcA), D-glucuronic acid methyl ester (MeGlcA), Allyl D-glucuronate (AllylGlcA) (**Figure 2-1**). They were purchased from Biosynth.

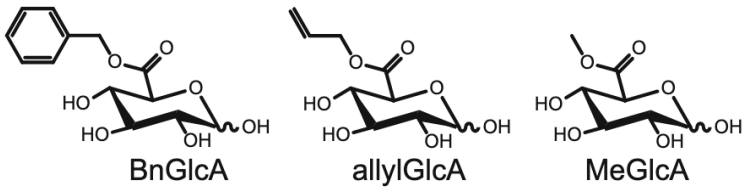

Figure 2-1. The structures of three model substrates used to detect glucuronoyl esterase activity (Hüttner, Klaubauf, et al., 2017).

2.2 Methods

2.2.1 Screening and obtaining glucuronoyl esterases from bacteria

In this study the potential GEs were screened from bacteria, each candidate was originated from different microorganisms and detailed information is shown in **Table 2-2**.

E. coli is easy to genetically manipulate, inexpensive to culture, and enables rapid protein expression, with recombinant proteins often produced within one day. Therefore, *E. coli* is a preferred host for recombinant protein expression (Francis & Page, 2010) and was selected as the expression host in this study. To promote the production of soluble proteins, the signal peptide and the linkage loop were removed from the full-length proteins, generating constructs designated as “nsp” (no signal peptide) and “nl” (no linkage loop), respectively.

Table 2-2. Detailed information of screened candidates

Candidate	Organism	Molecular Weight (MW)
CE15_2	*Marinimicrobium agarilyticum*	65 kDa
CE15_6	*Salegentibacter sp. Hel_I*	49 kDa
CE15_7	*Mariniblastus fucicola*	50 kDa
CE15_9	*Lentisphaerae bacterium*	70 kDa
CE15_13	*Bremerella cremea*	45 kDa
CE15_15	*Niastella populi*	46 kDa

2.2.1.1 Transformation

Plasmids were introduced into chemically competent *E. coli* cells by heat shock. Competent cells taken from -80°C were thawed on ice for 15 min. Plasmid, up to 100ng, was then added

to the cells, gently mixed, and incubated on ice for 30 min. The mixture was heated at 42°C for 45-90 s, immediately returned to ice for 2-10 mL. Next, 1 mL of LB medium was added, and the mixture was incubated at 37°C under shaking for 1 h to allow recovery. The cells were then plated onto LB agar plates containing 100 μg/mL ampicillin. Finally, the plates were incubated at 37°C overnight for less than 16 h. As shown in **Table 2-1** above, successful transformants were obtained, and single colonies were picked and streaked onto fresh LB plates with ampicillin to generate stock plates. These mother plates were subsequently used to inoculate cultures for downstream protein expression and purification.

2.2.1.2 Protein expression and purification

2.2.1.2.1 Inoculum preparation

A single colony was picked from the stock plate and inoculated into 3 mL LB medium supplemented with 100 μg/mL ampicillin in a 15 mL conical tube, followed by incubation at 37°C with shaking for 16 h as a pre-inoculum.

2.2.1.2.2 Cultivation and IPTG induction

The main culture was inoculated with 1% (v/v) of the pre-inoculum in 100-150 mL fresh LB medium containing ampicillin and cultivated at 37°C with shaking (200-220 rpm) until the OD_{600nm} reached 0.6–0.8 (typically after 2–3 h). Protein expression was induced by adding IPTG when the culture reached an OD_{600nm} of 0.6–0.8, which is commonly considered an appropriate growth phase for induction (Francis & Page, 2010). Next, the cultures were incubated at either 16 °C or 26 °C with shaking for approximately 20 h (overnight). Since the optimal expression conditions were successfully determined, protein expression was carried out under the established temperature and IPTG concentration conditions.

2.2.1.2.3 Protein extraction

Cells were harvested by centrifugation at 10,000 x g for 15 min to separate the supernatant and the cell pellet. The pellet was fully resuspended in 10 mL HEPES binding buffer. Then, sonication was performed at 30% amplitude with 30 s pulse followed by 30 s cooling intervals, for a total sonication time of 5 min to release intracellular proteins. The lysate was then centrifuged at 19,000 x g for 30 min to separate soluble proteins (supernatant) from insoluble material (pellet). Among the six candidate proteins, only CE15_6nl, CE15_13nl, and CE15_15nsp were successfully expressed in soluble form. The remaining candidates were mainly present, at the insoluble fraction probably due to formation of inclusion bodies. Thus, CE15_6nl, CE15_13nl, and CE15_15nsp were selected for downstream analyses.

2.2.1.2.4 Protein purification

Soluble proteins were purified using immobilized metal affinity chromatography (IMAC) purification on an ÄKTA start system. Supernatant was added into 1 mL HisTrap column from Cytiva, (packed nickel resin) and washed with the HEPES binding buffer (50 mM imidazole, 500 mM NaCI, 50 mM HEPES, 5% (v/v) Glycerol) to remove unspecific proteins. Target protein was eluted with the HEPES elution buffer (500 mM imidazole, 500 mM NaCI, 50 mM HEPES, 5% (v/v) Glycerol), and fractions were collected.

2.2.1.2.5 Dialysis

To exchange the buffer and remove imidazole and other small molecules, purified proteins were transferred into dialysis membrane with a molecular weight cut-off (MWCO) of 30 kDa and dialyzed against PBS overnight at 4°C with gentle magnetic stirring. After dialysis, the proteins were stored in PBS for subsequent experiments.

2.2.1.2.6 SDS-PAGE

Each protein sample (15 µL) was mixed with 5 µL SDS loading dye in 1.5 mL microcentrifuge tube, heat-denatured at 100°C for 10 min and then loaded onto an SDS-PAGE gel (Mini-PROTEAN TGX Stain-Free Precast Gels, 4-15 %) to assess protein expression and verify the presence of the target protein based on its expected molecular weight. The SDS-PAGE analysis of protein expression and purification was shown in **Figure 2-2**.

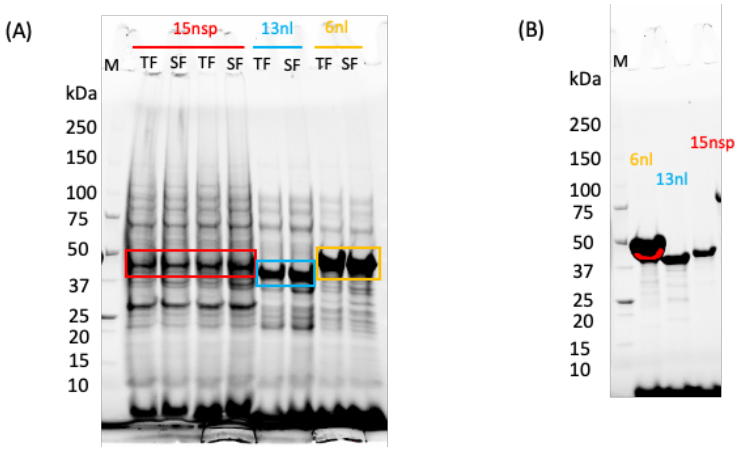

Figure 2-2. SDS-PAGE analysis of soluble expression and purified protein samples (A) Soluble expression of candidate recombinant proteins (TS refers to total fraction, and SF to soluble fraction). (B) Purified protein samples after dialysis.

2.2.1.3 Nanodrop and Bradford assay

To determine the concentration of proteins, nanodrop can provide quick measurements, whereas Bradford assay provides a more accurate estimation of protein concentration.

2.2.1.3.1 Nanodrop

After dialysis, protein concentration was estimated using a NanoDrop spectrophotometer. The instrument was blanked with water, and each purified protein sample was measured at 280 nm. The protein concentration was estimated from the absorbance at 280 nm using the protein A280 mode.

2.2.1.3.2 Bradford assay

The Bradford assay was used to determine accurate protein concentration. A standard curve was prepared using bovine serum albumin (BSA) standards ranging from 0 to 1 mg/mL. The standards and diluted protein samples were mixed with Bradford reagent and incubated at room temperature for 5 min. A mixture of PBS and Bradford reagent was used as the blank control. Absorbance was measured at 595 nm using a spectrophotometer and 1 mL cuvettes. The protein

concentration of each sample was calculated from the BSA standard curve. A representative BSA standard curve is shown in Appendix **Figure 8-1**.

2.2.2 Analysis of biochemical characterization of purified proteins

2.2.2.1 nanoDifferential Scanning fluorimetry (nanoDSF)

Purified proteins were diluted to 0.2 mg/mL in 50 µL of McIlvaine buffer at varying pH values (pH 3.2, 4.4, 5.6, 6.0, 6.5, 7.0, 7.5, 8.0). The pH 9.0 buffer was prepared using CHES (N-Cyclohexyltaurine) and adjusted to pH 9.0 with NaOH. Preparation details in Appendix **Table 8-1**), and 10 µL of each sample was loaded into capillaries. The intrinsic fluorescence at 330 nm and 350 nm was monitored using a Prometheus NT 48 nanoDSF (NanoTemper Technologies, Germany) while the temperature was increased from 20 °C to 90 °C at a rate of 1 °C per minute. Data were analyzed using PR. Therm.Control software (Version 2.0, Germany), and the melting temperature (T_m) was determined from the first derivative of the 350/330 nm fluorescence ratio.

2.2.2.2 Stability in storage

Esterase activity was monitored continuously using the K-URONIC kit, in which uronic acid formation was coupled to NADH production and detected by measuring the increase in absorbance at 340 nm. Kinetic measurements were conducted in 96-well plates with a Multiskan GO Microplate Spectrophotometer (Thermo Fisher Scientific, Finland) in 70 µL reactions, consisting of a 50 µL coupled reaction system (20 µL NAD^+, 20 µL pH 8.0 buffer, 2 µL uronate dehydrogenase (UDH), and 8 µL MilliQ water) and a 20 µL enzymatic reaction system (**Table 2-3**). The model substrates BnzGlcA, AllylGlcA, and MeGlcA were dissolved in 100% DMSO, with a final DMSO concentration of ≤10% in all reactions. Assays were performed in triplicate at 30 °C for CE15_13nl and CE15_15nsp, and at 40°C for CE15_6nl, using sufficient enzyme amounts to ensure a ≥ 2-fold increase in substrate turnover over autohydrolysis rates.

To evaluate storage stability at 4°C, purified enzymes were assayed at multiple time points using identical conditions and equal enzyme amounts. Specific activity measured on day 0 was set as 100%, and subsequent measurements were expressed as relative residual activity (%). The residual activity was calculated as below:

$$\text{Residual Activity (\%)} = \frac{\text{specific activity at each time point}}{\text{specific activity at Day 0}} \times 100$$

Table 2-3. Composition of the coupled continuous assay mixture used for glucuronoyl esterase activity measurements.

	Reagent	Sample	Blank	Standard solution
Coupled reaction system	NAD^+	20	20	20
	pH 8.0 buffer	20	20	20

	UDH	2	2	2
	MilliQ-water	8	8	8
Enzymatic reaction system	Enzyme	5	-	-
	Substrate	5	5	-
	PBS	-	5	5
	4-O-MeGlcA STD*	-	-	5
	pH 7.0 buffer	10	10	10

* GlcA STD: 4-O-Methyl-D-glucuronic Acid standard solution

2.2.3 Enzymatic activity and kinetic analysis on model substrates

Enzymatic activity toward model substrates was measured using the standard activity assay described above. For kinetic analysis, at least seven substrate concentrations were tested for each model substrate. Initial rates were calculated from the linear range of product formation and fitted to the Michaelis–Menten equation to estimate K_m, V_{max}, and k_{cat}, where applicable.

A standard curve was generated using gradient concentrations of 4-O-MeGlcA standard solution (0, 1, 2, 3, 4, 5 mM). The standards were measured using the same coupled enzymatic assay, and absorbance at 340 nm was used to quantify the relationship between uronic acid and absorbance in the enzyme reactions.

2.2.4 Enzymatic activity on complex substrate

2.2.4.1 Sequential enzymatic reaction on corn bran

A sequential enzymatic reaction was performed to evaluate the effect of GEs on corn bran degradation and on the subsequent hydrolysis by GH30. Corn bran was prepared at a final concentration of 1% (w/v) in McIlvaine buffer at pH 6.5 for CE15_6nl or pH 7.0 for CE15_13nl and 15nsp. GEs were added at a final concentration of 0.1 g/L, and the final reaction volume was adjusted with the corresponding pH buffer.

In the first reaction step, CE15_6nl was incubated with corn bran at 45°C, whereas CE15_13nl and CE15_15nsp were incubated at 38°C, based on the optimal pH conditions determined by nanoDSF. All reactions were performed under shaking. 100 µL samples were collected at 0, 1, 3, 6, 12, 24, and 48 h and immediately inactivated by 100°C heating for 5 min. Reactions containing corn bran and the corresponding buffer without enzyme were used as controls.

In the second reaction step, 50 µL of each heat-inactivated sample from the first reaction was further incubated with 0.01g/L GH30 (NZYtech). The reactions were carried out at 38°C under shaking for 12 h. Control reactions for the second step contained GH30 and corn bran, and they were collected at 0 h and 12 h.

2.2.4.2 Analysis of products by HPAEC-PAD

Sample preparation

After enzymatic hydrolysis reactions, all samples from both reactions were diluted 20-fold in Milli-Q water and filtered through 0.22 μm polypropylene (PES) filters (Sarstedt, Germany) before conducting the HPAEC-PAD.

Analysis of HPAEC-PAD

The products from sequential enzymatic reactions were analyzed by HPAEC-PAD (ICS-6000, Dionex, Thermo Fisher Scientific, USA). Product separation was achieved by injecting 10 μL of sample onto the HPAEC-PAD system consisting of a Dionex CarboPac PA-200 analytical column (250 mm × 3 mm, 5.5 μm particle size) equipped with a guard column (50 mm × 3 mm) (Thermo Scientific). An ED40 electro-chemical detector (Thermo Fisher Scientific) was used to detect analytes, and the reference electrode was in PdH mode. Separation was achieved using three eluents: eluent A (Milli-Q water), eluent B (NaOH and NaOAc), and eluent C (NaOH) for a total analysis time of 23 min.

3 Results

3.1 Determination of protein thermal stability

To evaluate enzyme thermostability under different pH conditions, nanoDSF assays were performed across a range of pH values. The result showed that CE15_6nl and CE15_15nsp reached their highest melting temperature (T_m) values at pH 7.0 and pH 6.5, with T_m values of 50.2 ± 0.0°C and 44.25 ± 0.05°C, respectively, indicating they were most stable under these pH conditions. However, CE15_13nl displayed the highest T_m at pH 9.0 (51.65 ± 0.15°C), suggesting that this enzyme was more stable under alkaline conditions (**Table 3-1**).

Table 3-1. Melting temperatures of enzymes measured by NanoDSF.

pH	CE15_6nl	CE15_13nl	CE15_15nsp
3.2	ND	ND	ND
4.4	ND	32.45±0.55	ND
5.6	42.6 ± 0.0	38.7±0.5	41.8±0.1
6	46 ± 0.0	41.35±0.05	43.45±0.05
6.5	48.15 ± 0.05	43.3±0.2	**44.25±0.05**
7	**50.2 ± 0.0**	45.25±0.15	44.1±0.1
7.5	49.9 ± 0.05	46.45±0.05	43.35±0.05
8	49.1 ± 0.0	46.9±0.0	42.25±0.05
9	45.4 ± 0.0	**51.65±0.15**	39.15±0.05

3.2 Verification of glucuronoyl esterase activity

Before further biochemical characterization, the glucuronoyl esterase activity of the purified proteins was verified firstly. CE15 enzymes catalyze hydrolysis of substrates, GlcA was released after the CE15 treatment of model substrates. Coupled continuous activity assays were conducted using both active proteins and their corresponding inactive proteins. For CE15_6nl,

the reaction was performed at 40°C, and this measurement was performed at 30°C for CE15_13nl and CE15_15nsp. The concentration of GlcA significantly increased at the initial reaction stage (**Figure 3-1**). As expected, active proteins showed detectable GE activity and the inactive proteins exhibited no or less activity under the identical reaction conditions. These results confirmed that the purified candidate proteins were active GEs which can be used for further biochemical characterization.

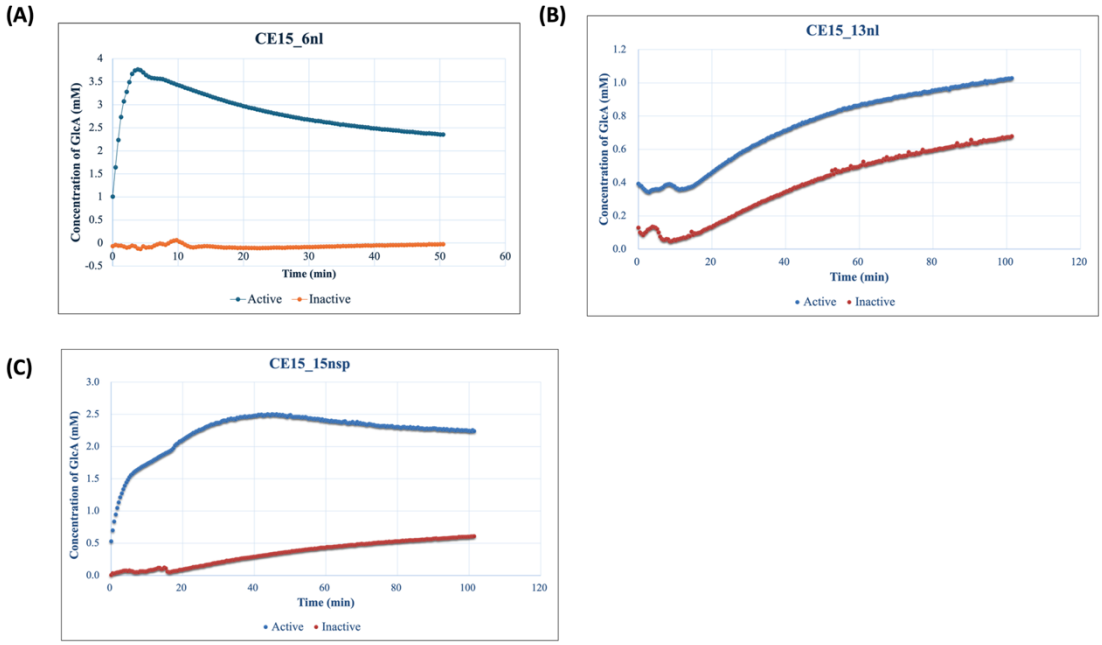

Figure 3-1. Detectable GE activity for CE15_6nl, CE15_13nl, and CE15_15nsp. The relationship between the concentration of GlcA that CE15 enzymes produced and minutes. (A) CE15_6nl (B) CE15_13nl (C) CE15_15nsp.

3.3 Storage stability

After dialysis, the purified enzymes were stored in PBS buffer at 4°C. To evaluate storage stability, the residual activities of CE15_13nl and CE15_15nsp were measured at Day 0, 4, 7, 14, and 21, while CE15_6nl was measured at Day 1, 7, and 14, using the K-URONIC kit with MeGlcA as the substrate. Among these enzymes, CE15_6nl and CE15_13nl showed better storage stability. Their specific activities fluctuated during the storage period. For these variations, they were likely due to instrument or reagent related errors. However, CE15_6nl and 13nl retained full active after 14 days (184.5% and 101.5%, respectively), indicating stable catalytic activity under refrigerated storage conditions and could be stored at 4°C for at least 14 days without obvious activity loss. Of note, CE15_13nl still maintained full activity at Day21 (153.9%), with residual activity even higher.

However, CE15_15nsp exhibited a relatively dramatic decrease in residual activity during the early stage of storage. Its residual activity decreased from 100% to 62.6% after 4 days, suggesting that the partial catalytic activity was lost during the initial storage period. However, after Day4, the activity remained relatively stable, fluctuating between approximately 62% and 73% from day 4 to day 14. The catalytic activity was lost close to 50% at Day21. Therefore,

CE15_15nsp was less stable than CE15_6nl, and 13nl during storage, but the remaining active enzyme fraction was relatively stable after 4 days (**Figure 3-2**).

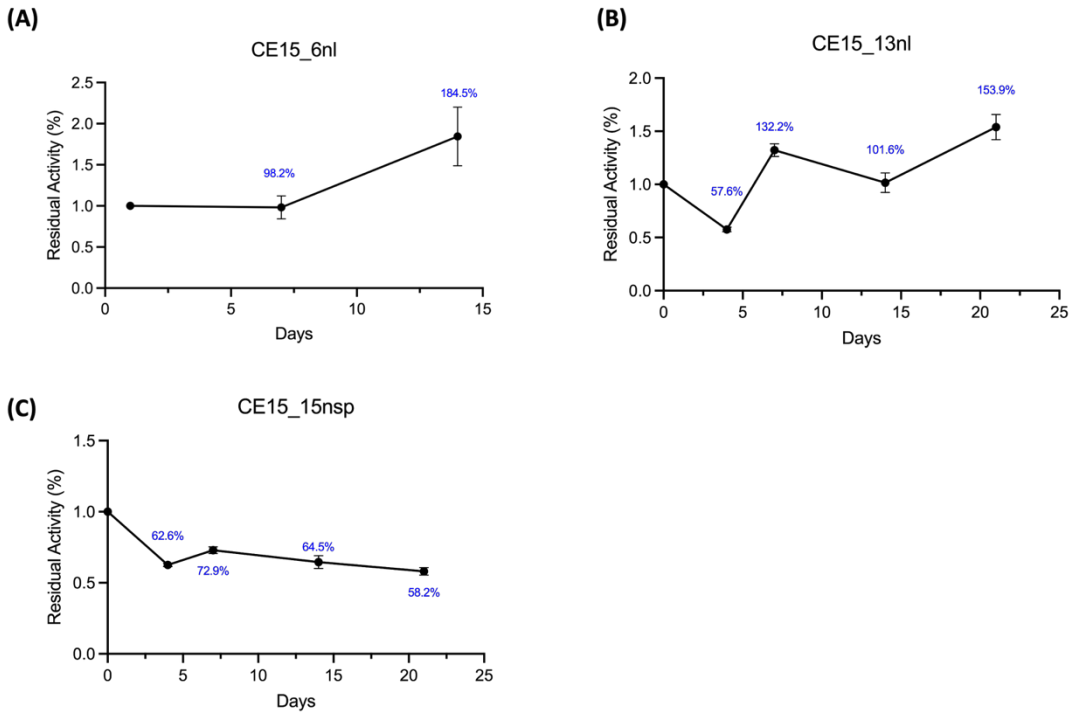

Figure 3-2. Storage stability of CE15_6nl, 13nl, and 15nsp for 14 days. Specific activity was measured at Day0, Day4, Day 7, and Day14. Residual activity was calculated based on the specific activity at Day0. (A) Storage stability of CE15_6nl. (B) Storage stability of CE15_13nl. (C) Storage stability of CE15_15nsp.

3.4 Biochemical characterization and substrate specificity of CE15 enzymes

Enzyme activity assays of CE15_6nl and CE15_15nsp were performed using three model substrates, BnzGlcA, MeGlcA, and AllylGlcA, and kinetic parameters were determined where possible (**Table 3-2**). K_m represents the substrate concentration at which the reaction velocity reaches half of V_{max}, which provides insight into the apparent affinity between an enzyme and its substrate. The K_m values of CE15_6nl and CE15_15nsp on BnzGlcA were lower than those on MeGlcA, suggesting that both enzymes had higher apparent affinity for BnzGlcA than for MeGlcA. The K_m values on AllylGlcA could not be determined since AllylGlcA saturation was not achieved up to 50 mM (Appendix **Figure 8-2**).

In addition, CE15_6nl showed comparable catalytic efficiencies toward the three substrates, suggesting limited discrimination toward the alcohol moiety. By contrast, CE15_15nsp exhibited a more pronounced preference depending on the alcohol moiety. The k_{cat}/K_m values of CE15_6nl were in the range of 10^3 M^{-1} s^{-1}, whereas those of CE15_15nsp toward BnzGlcA were approximately two orders of magnitude higher than AllylGlcA (**Table 3-2**). These results suggested that CE15_6nl and 15nsp enzymes were not strict with methyl derivatives, but

CE15_15nsp showed significant discrimination toward the alcohol moiety.

Table 3-2. Kinetic parameters of CE15_6nl and 15nsp on various model substrates.

Enzyme	Substrate	K_m (mM)	k_{cat} (s^{-1})	k_{cat}/K_m ($s^{-1}M^{-1}$)
CE15_6nl	BnzGlcA	11.18 ± 1.28	88.96 ± 6.67	(7.78 ± 0.34) x 10^3
	AllylGlcA	*Cannot be saturated up to 50 mM*		(2.79 ± 0.15) x 10^3
	MeGlcA	14.01 ± 0.31	106.17	(7.58 ± 0.17) x 10^3
CE15_15nsp	BnzGlcA	1.28 ± 0.24	27.4 ± 1.79	(2.154 ± 2.6) x 10^4
	AllylGlcA	*Cannot be saturated up to 50 mM*		(7.92 ± 1.02) x 10^2
	MeGlcA	3.195	63.02	1.972 x 10^4

3.5 Analysis of enzymatic activity on pretreated corn bran

3.5.1 Hydrolysis action pretreated corn bran by individual CE15 enzymes

Corn bran is mainly composed of cellulose, hemicellulose, and lignin. Alkaline pretreatment of corn bran and fresh CE15_6nl, 13nl and 15nsp were used in this study. The enzymatic reactions were performed at 45 °C for CE15_6nl and 38 °C for 13nl and 15nsp theoretically, but in practical, the reactions of CE15_13nl and 15nsp were conducted at 34.5 °C. HPAEC analysis of reaction products clearly demonstrated that three CE15 enzymes could generate xylooligosaccharides (XOS) from pretreated corn bran residues, but the intensity and profile of product peaks generated by three CE15 enzymes were different. In detail, the highest intensity of unidentified product retention time between 4.1-4.4 min was produced by CE15_15nsp, followed by 13nl and 6nl at both time points (**Figure 3-3**), which area were 0.1363, 0.3580, and 2.3736, indicating that the accumulation of this product in CE15_15nsp was higher than others. In addition, the catalytic efficiency of CE15_15nsp against model substrates was the highest, suggesting that model substrates may serve as relevant screening candidates to identify relevant enzymes. Moreover, they all showed no release of other linear XOS except small amount of X3 and X4 after reaction for 48 hours compared to the control and the peak profile at 0 h.

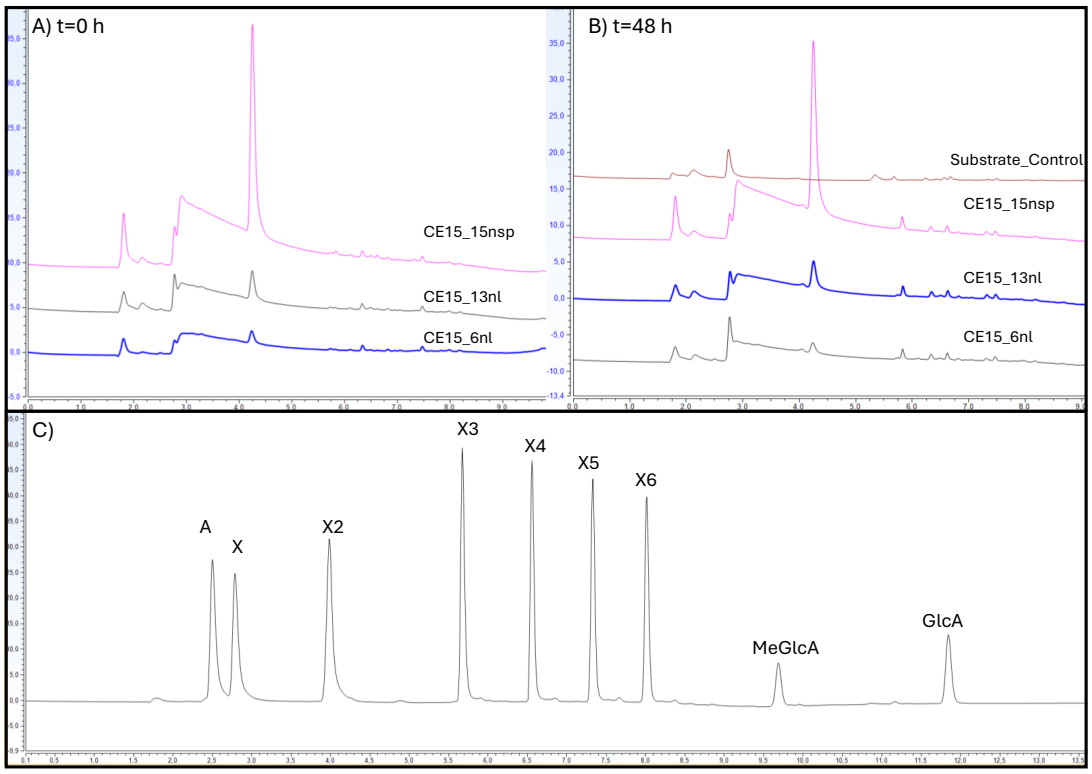

Figure 3-3. HPAEC-PAD analysis of product profile generated by CE15s from pretreated corn bran residues. (A) CE15_6nl, 13nl, and 15nsp were inactivated at t = 0 h. (B) CE15_6nl, 13nl, and 15nsp were inactivated at t = 48 h. (C) AXOS standards consists of arabinose, xylose, xylobiose (X2), xylotriose (X3), xylotetraose (X4), xylopentaose (X5), xylohexaose (X6), 4-O-methyl-D-glucuronic acid (MeGlcA), and D-glucuronic acid (GlcA).

3.5.2 Synergetic effect of GEs and GH30 on pretreated corn bran

BoXyn30A (GH30_8) enzyme from *Bacteroides ovatus* mainly produced monomeric xylose and glucuronic acid-substituted xylooligsaccharides (GXOSs) (Salas-Veizaga et al., 2021). The combination of GEs and GH11 xylanase showed an increased saccharification of X1-X6 sugars (Pentari et al., 2025). To explore the synergistic effect of GEs and GH30, after GEs treatment of substrate, 0.01g/L GH30 was added into reaction systems taken from the previous treatment at each time point, and the reactions were performed at 38°C for 12 h. However, no clear synergetic effect was observed from three GEs and GH30, as the product profile of *BoXyn30A* against GE-treated corn bran substrate (Substrate + GH30) and samples (CE15 + GH30) exhibited no difference from **Figure 3-4**.

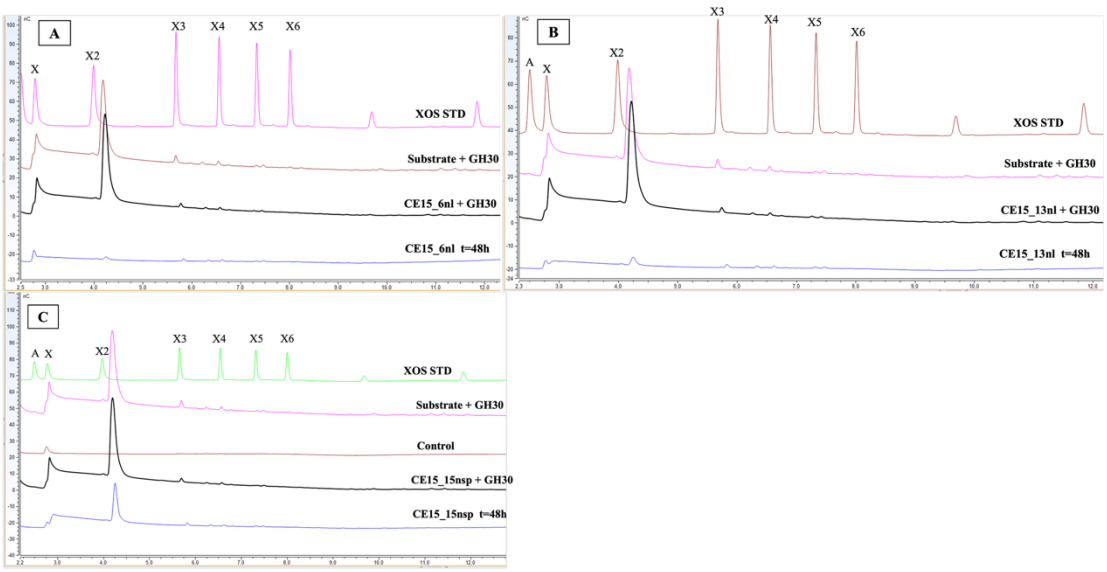

Figure 3-4. HPAEC-PAD chromatogram of *BoXyn30A* product profile against CE15 enzymes-treated corn bran biomass. Substrate represented CE15 enzymes-treated corn bran biomass for 48 hours. (A) CE15_6nl; (B) CE15_13nl; (C) CE15_15nsp.

4 Discussion

The hydrolysis of ester bonds between lignin and carbohydrates by glucuronoyl esterases have been observed from both bacterial and fungal microorganisms. Several fungal and bacterial CE15 enzymes have been found and characterized for their kinetic parameters and substrate specificity. Thermal stability of the CE15 enzymes was assessed prior to biochemical characterization. As expected, CE15_6nl and CE15_15nsp showed the highest T_m (50.2 ± 0.0°C and 44.25 ± 0.05°C, respectively) at neutral and slightly acidic conditions, while CE15_13nl exhibited a higher T_m (51.65 ± 0.15°C) under alkaline conditions, suggesting that it is an alkaline-tolerant enzyme (**Table 3-1**). Previous study showed that the T_m values below the optimal growth temperature of the bacterium may be attributed to the absence of glycosylation (Chung et al., 2015). In this study, their T_m values were higher than optimal growth temperatures of the native hosts of CE15_6nl, 13nl, and 15nsp were 12, 30, and 30°C, respectively, indicating recombinant enzymes were thermally stable after heterologous expression in *E. coli*. Together with their soluble expression and successful purification, these results support the suitability of these proteins for further biochemical characterization.

By comparing identified fungal and bacterial GEs, they have common biochemical characterizations. Generally, they have preference on bulkier substrates due to the complicated structure of native LCCs. Several bacterial CE15 enzymes have been reported to display substrate preferences related to the alcohol moiety. For instance, OtCE15C showed higher catalytic efficiency toward BnzGlcA than toward MeGlcA and AllylGlcA (Arnling Bååth et al., 2018a). Moreover, the catalytic efficiencies of bacterial CE15 enzymes are often 10- to 100-fold higher than those reported for fungal GEs (d'Errico et al., 2015; De Santi et al., 2016; Huynh et al., 2018). Consistent with these observations, CE15_6nl and CE15_15nsp showed their highest kcat/Km values toward BnzGlcA among the tested substrates, with values of (7.78 ± 0.34) × 10^3 and (2.154 ± 2.6) × 10^4 M^{-1} s^{-1}, respectively (**Table 3-2**). This indicates that these

enzymes exhibited higher catalytic efficiency toward the substrate with a bulkier alcohol moiety. CE15_13nl showed relatively low catalytic efficiency compared to the other two CE15 enzymes when assayed with model substrates at 30°C (data not shown). Since its T_m continued to increase up to pH 9.0, the optimal T_m was not determined. As previous reports have suggested that enzymes tend to show higher activity at temperatures close to their T_m (Krska & Larsbrink, 2020), the kinetic parameters of CE15_13nl should be investigated under 30°C or other conditions (Krska & Larsbrink, 2020). However, substrate specificity differs notably between bacterial and fungal GEs. Bacterial GEs are not strict toward methyl derivatives on glucuronic acid and can act on substrates lacking 4-O-methylation, whereas 4-O-methylation is essential for fungal GE activity (d'Errico et al., 2015; Špániková et al., 2007).

Furthermore, bacterial GEs showed activity toward galacturonate esters, whereas fungal GEs showed no detectable activity on these substrates (Arnling Bååth et al., 2018b), suggesting that bacterial GEs may have wider substrate specificity. In this study, glucuronate esters without methylation were used to detect GE activity, and all three CE15 enzymes showed measurable activity compared to the inactive enzyme controls (**Figure 3-1**). The storage stability of CE15 enzymes at 4°C was evaluated, as maintaining enzyme integrity is essential for reliable determination of kinetic parameters. CE15_6nl and CE15_13nl retained stable catalytic activity for at least 14 days, whereas CE15_15nsp showed activity loss around 40% by Day 4 (**Figure 3-2**). The expression of CE15 genes was upregulated when microorganisms were grown on complex biomass compared to glucose or yeast extract (Hüttner, Nguyen, et al., 2017; MacDonald et al., 2011), suggesting that CE15 enzyme activity is likely induced by biomass. GEs have been shown to improve enzymatic saccharification of corn fiber, release xylooligosaccharides from LCC extracts of birch wood, and act synergistically with xylanases (d'Errico et al., 2016; Mosbech et al., 2018a).

Consistent with these findings, single CE15 enzymes in this study also promoted the release of XOS (**Figure 3-3**). LCC-cleaving activity may be particularly important during the initial stages of intact biomass hydrolysis, where GEs likely enhance the accessibility of other glycolytic enzymes to polysaccharides within the complex plant cell wall matrix. A tight functional relationship between GEs and xylanases has been postulated, where GEs act either prior to or in concert with endo-xylanases to detach xylan from lignin, or release xylanase-generated XOS from lignin networks for further degradation into monosaccharides. Report shown that synergistic cooperation between a fungal GE and xylanases (Mosbech et al., 2018b). However, the synergistic effects between a GH30 xylanase and three CE15 enzymes were not observed in this study (**Figure 3-4**).

5 Conclusion

In conclusion, bacterial glucuronoyl esterases from the CE15 family were screened and successfully obtained as purified proteins through heterologous expression. Thermal stability of the CE15 enzymes was assessed by nanoDSF, and kinetic parameter determination of CE15_6nl and CE15_15nsp highlighted a preference for larger substrates. The effects of bacterial GEs on corn bran biomass support the proposed role of these enzymes in reducing lignocellulose recalcitrance, as evidenced by the increased release of XOS.

6 Acknowledgment

As I am writing this, I realize everything has to come to an end eventually. Time flies so fast. It still feels like I just joined the division of biotechnology back in September 2025, and now it is already the end of May.

First of all, I want to say a huge thanks to my supervisor, Savvina Leontakianakou. She patiently taught me lab skills and academic knowledge and always encouraged me to keep going. Whenever I had thought or questions, she listened carefully and supported me. Her warm, kind smile always cheered me up. She is like a little sun to me. I have learned so much from her. She stays positive about life and takes her work seriously and responsibly, because she truly loves research. I always gain something new every time I talk with her. People with warm hearts keep spreading their warm to everyone around them, just like her.

I would also like to thank my examiner, Eva Nordberg Karlsson. Thank you for giving me the opportunity to complete my advanced course and master's thesis. She provided me with many practical ideas and suggestions for my project. It has been my great honor to complete my studies within the Fermentation Group. I also want to thank Roya Sardari. She is such a warm-hearted person. She always pays close attention to my safety in the lab and kindly reminds me of important precautions. She offers help whenever I need it, and even with equipment she is not familiar with, she does her best to support me. She also occasionally shares little snacks with us, which makes our lab time much nicer. My gratitude also goes to everyone in the Fermentation Group: Andrius Jasilionis, Israt Jahan Mukti, Christina Wennerberg, Annika Malmgren, Mariel Perez Zabaleta, and Sebastian Kempengren. I am thankful for every moment we spent together.

Thank you to everyone in the Biotechnology Division!

I am also grateful for all the friends I have met in Sweden. You have made my life here so colorful, and I will always remember the Spring Festival and every holiday we spent together.

Special thanks go to my lab partner and friend Rithika Vivekananda Nayak. We share many similar views in life, exchange our thoughts and feelings, and always encourage and support each other. I am truly thankful for meeting you.

Finally, I would like to thank my family for all their continuous support.

7 References

Agbor, V. B., Cicek, N., Sparling, R., Berlin, A., & Levin, D. B. (2011). Biomass pretreatment: Fundamentals toward application. *Biotechnology Advances*, *29*(6), 675–685. https://doi.org/10.1016/j.biotechadv.2011.05.005

Agger, J. W., Madsen, M. S., Martinsen, L. K., Martins, P. A., Barrett, K., & Meyer, A. S. (2023). New insights to diversity and enzyme–substrate interactions of fungal glucuronoyl esterases. *Applied Microbiology and Biotechnology*, *107*(14), 4447–4457. https://doi.org/10.1007/s00253-023-12575-4

Arnling Bååth, J., Giummarella, N., Klaubauf, S., Lawoko, M., & Olsson, L. (2016a). A glucuronoyl esterase from *Acremonium alcalophilum* cleaves native lignin-carbohydrate ester bonds. *FEBS Letters*, *590*(16), 2611–2618. https://doi.org/10.1002/1873-3468.12290

Arnling Bååth, J., Giummarella, N., Klaubauf, S., Lawoko, M., & Olsson, L. (2016b). A glucuronoyl esterase from *Acremonium alcalophilum* cleaves native lignin-carbohydrate ester bonds. *FEBS Letters*, *590*(16), 2611–2618. https://doi.org/10.1002/1873-3468.12290

Arnling Bååth, J., Mazurkewich, S., Knudsen, R. M., Poulsen, J.-C. N., Olsson, L., Lo Leggio, L., & Larsbrink, J. (2018a). Biochemical and structural features of diverse bacterial glucuronoyl esterases facilitating recalcitrant biomass conversion. *Biotechnology for Biofuels*, *11*, 213. https://doi.org/10.1186/s13068-018-1213-x

Arnling Bååth, J., Mazurkewich, S., Knudsen, R. M., Poulsen, J.-C. N., Olsson, L., Lo Leggio, L., & Larsbrink, J. (2018b). Biochemical and structural features of diverse bacterial glucuronoyl esterases facilitating recalcitrant biomass conversion. *Biotechnology for Biofuels*, *11*(1), 213. https://doi.org/10.1186/s13068-018-1213-x

Arnling Bååth, J., Mazurkewich, S., Poulsen, J.-C. N., Olsson, L., Lo Leggio, L., & Larsbrink, J. (2019). Structure–function analyses reveal that a glucuronoyl esterase from Teredinibacter turnerae interacts with carbohydrates and aromatic compounds. *Journal of Biological Chemistry*, *294*(16), 6635–6644. https://doi.org/10.1074/jbc.RA119.007831

Aulin, C., Ahola, S., Josefsson, P., Nishino, T., Hirose, Y., Österberg, M., & Wågberg, L. (2009). Nanoscale Cellulose Films with Different Crystallinities and Mesostructures—Their Surface Properties and Interaction with Water. *Langmuir*, *25*(13), 7675–7685. https://doi.org/10.1021/la900323n

Balakshin, M., Capanema, E., Gracz, H., Chang, H., & Jameel, H. (2011). Quantification of lignin–carbohydrate linkages with high-resolution NMR spectroscopy. *Planta*, *233*(6), 1097–1110. https://doi.org/10.1007/s00425-011-1359-2

Balan, V., Sousa, L. D. C., Chundawat, S. P. S., Marshall, D., Sharma, L. N., Chambliss, C. K., & Dale, B. E. (2009). Enzymatic digestibility and pretreatment degradation products of AFEX-treated hardwoods (*Populus nigra*). *Biotechnology Progress*, *25*(2), 365–375. https://doi.org/10.1002/btpr.160

Barakat, A., De Vries, H., & Rouau, X. (2013). Dry fractionation process as an important step in current and future lignocellulose biorefineries: A review. *Bioresource Technology*, *134*, 362–373. https://doi.org/10.1016/j.biortech.2013.01.169

Bauer, S., Vasu, P., Persson, S., Mort, A. J., & Somerville, C. R. (2006). Development and application of a suite of polysaccharide-degrading enzymes for analyzing plant cell walls. *Proceedings of the National Academy of Sciences*, *103*(30), 11417–11422. https://doi.org/10.1073/pnas.0604632103

Biely, P., Puchart, V., Stringer, M. A., & Mørkeberg Krogh, K. B. R. (2014). *Trichoderma reesei* XYN VI – a novel appendage-dependent eukaryotic glucuronoxylan hydrolase. *The FEBS Journal*, *281*(17), 3894–3903. https://doi.org/10.1111/febs.12925

Brethauer, S., Shahab, R. L., & Studer, M. H. (2020). Impacts of biofilms on the conversion of cellulose. *Applied Microbiology and Biotechnology*, *104*(12), 5201–5212. https://doi.org/10.1007/s00253-020-10595-y

Brethauer, S., & Wyman, C. E. (2010). Review: Continuous hydrolysis and fermentation for cellulosic ethanol production. *Bioresource Technology*, *101*(13), 4862–4874. https://doi.org/10.1016/j.biortech.2009.11.009

Chen, H. (2014a). Chemical Composition and Structure of Natural Lignocellulose. In H. Chen, *Biotechnology of Lignocellulose* (pp. 25–71). Springer Netherlands. https://doi.org/10.1007/978-94-007-6898-7_2

Chen, H. (2014b). Chemical Composition and Structure of Natural Lignocellulose. In H. Chen, *Biotechnology of Lignocellulose* (pp. 25–71). Springer Netherlands. https://doi.org/10.1007/978-94-007-6898-7_2

Chung, D., Young, J., Bomble, Y. J., Vander Wall, T. A., Groom, J., Himmel, M. E., & Westpheling, J. (2015). Homologous Expression of the Caldicellulosiruptor bescii CelA Reveals that the Extracellular Protein Is Glycosylated. *PLOS ONE*, *10*(3), e0119508. https://doi.org/10.1371/journal.pone.0119508

d'Errico, C., Börjesson, J., Ding, H., Krogh, K. B. R. M., Spodsberg, N., Madsen, R., & Monrad, R. N. (2016). Improved biomass degradation using fungal glucuronoyl—Esterases—Hydrolysis of natural corn fiber substrate. *Journal of Biotechnology*, *219*, 117–123. https://doi.org/10.1016/j.jbiotec.2015.12.024

d'Errico, C., Jørgensen, J. O., Krogh, K. B. R. M., Spodsberg, N., Madsen, R., & Monrad, R. N. (2015). Enzymatic degradation of lignin-carbohydrate complexes (LCCs): Model studies using a fungal glucuronoyl esterase from *Cerrena unicolor*. *Biotechnology and Bioengineering*, *112*(5), 914–922. https://doi.org/10.1002/bit.25508

De Santi, C., Willassen, N. P., & Williamson, A. (2016). Biochemical Characterization of a Family 15 Carbohydrate Esterase from a Bacterial Marine Arctic Metagenome. *PloS One*, *11*(7), e0159345. https://doi.org/10.1371/journal.pone.0159345

Ďuranová, M., Hirsch, J., Kolenová, K., & Biely, P. (2009). Fungal Glucuronoyl Esterases and Substrate Uronic Acid Recognition. *Bioscience, Biotechnology, and Biochemistry*, *73*(11), 2483–2487. https://doi.org/10.1271/bbb.90486

Eriksson, □., Goring, D. A. I., & Lindgren, B. O. (1980). Structural studies on the chemical bonds between lignins and carbohydrates in spruce wood. *Wood Science and Technology*, *14*(4), 267–279. https://doi.org/10.1007/BF00383454

Francis, D. M., & Page, R. (2010). Strategies to Optimize Protein Expression in *E. coli*. *Current Protocols in Protein Science*, *61*(1). https://doi.org/10.1002/0471140864.ps0524s61

Gandini, A. (2011). The irruption of polymers from renewable resources on the scene of macromolecular science and technology. *Green Chemistry*, *13*(5), 1061.

https://doi.org/10.1039/c0gc00789g

Gavande, P. V., Goyal, A., & Fontes, C. M. G. A. (2023). Carbohydrates and Carbohydrate-Active enZymes (CAZyme): An overview. In *Glycoside Hydrolases* (pp. 1–23). Elsevier. https://doi.org/10.1016/B978-0-323-91805-3.00012-5

Gibson, L. J. (2012). The hierarchical structure and mechanics of plant materials. *Journal of The Royal Society Interface*, *9*(76), 2749–2766. https://doi.org/10.1098/rsif.2012.0341

Henrissat, B. (1991). A classification of glycosyl hydrolases based on amino acid sequence similarities. *Biochemical Journal*, *280*(2), 309–316. https://doi.org/10.1042/bj2800309

Henrissat, B., & Bairoch, A. (1993). New families in the classification of glycosyl hydrolases based on amino acid sequence similarities. *Biochemical Journal*, *293*(3), 781–788. https://doi.org/10.1042/bj2930781

Henrissat, B., Claeyssens, M., Tomme, P., Lemesle, L., & Mornon, J.-P. (1989). Cellulase families revealed by hydrophobic cluster analysi. *Gene*, *81*(1), 83–95. https://doi.org/10.1016/0378-1119(89)90339-9

Himmel, M. E., Ding, S.-Y., Johnson, D. K., Adney, W. S., Nimlos, M. R., Brady, J. W., & Foust, T. D. (2007). Biomass Recalcitrance: Engineering Plants and Enzymes for Biofuels Production. *Science*, *315*(5813), 804–807. https://doi.org/10.1126/science.1137016

Hüttner, S., Klaubauf, S., De Vries, R. P., & Olsson, L. (2017). Characterisation of three fungal glucuronoyl esterases on glucuronic acid ester model compounds. *Applied Microbiology and Biotechnology*, *101*(13), 5301–5311. https://doi.org/10.1007/s00253-017-8266-9

Hüttner, S., Nguyen, T. T., Granchi, Z., Chin-A-Woeng, T., Ahrén, D., Larsbrink, J., Thanh, V. N., & Olsson, L. (2017). Combined genome and transcriptome sequencing to investigate the plant cell wall degrading enzyme system in the thermophilic fungus Malbranchea cinnamomea. *Biotechnology for Biofuels*, *10*(1), 265. https://doi.org/10.1186/s13068-017-0956-0

Huynh, H. H., Ishii, N., Matsuo, I., & Arioka, M. (2018). A novel glucuronoyl esterase from Aspergillus fumigatus—The role of conserved Lys residue in the preference for 4-O-methyl glucuronoyl esters. *Applied Microbiology and Biotechnology*, *102*(5), 2191–2201. https://doi.org/10.1007/s00253-018-8739-5

Jin, Z., Katsumata, K. S., Lam, T. B. T., & Iiyama, K. (2006). Covalent linkages between cellulose and lignin in cell walls of coniferous and nonconiferous woods. *Biopolymers*, *83*(2), 103–110. https://doi.org/10.1002/bip.20533

Krska, D., & Larsbrink, J. (2020). Investigation of a thermostable multi-domain xylanase-glucuronoyl esterase enzyme from Caldicellulosiruptor kristjanssonii incorporating multiple carbohydrate-binding modules. *Biotechnology for Biofuels*, *13*(1), 68. https://doi.org/10.1186/s13068-020-01709-9

Laine, R. A. (1994). Invited Commentary: A calculation of all possible oligosaccharide isomers both branched and linear yields 1.05×10^{12} structures for a reducing hexasaccharide: the *Isomer Barrier* to development of single-method saccharide sequencing or synthesis systems. *Glycobiology*, *4*(6), 759–767. https://doi.org/10.1093/glycob/4.6.759

Lam, T. B. T., & Iiyama, K. (2000). Characteristics of senescent straw cell walls of dwarf, semidwarf, and normal strains of rice (Oryza sativa) plants. *Journal of Wood Science*,

46(5), 376–380. https://doi.org/10.1007/BF00776399

Larsbrink, J., & Lo Leggio, L. (2023). Glucuronoyl esterases—Enzymes to decouple lignin and carbohydrates and enable better utilization of renewable plant biomass. *Essays in Biochemistry*, *67*(3), 493–503. https://doi.org/10.1042/EBC20220155

Laureano-Perez, L., Teymouri, F., Alizadeh, H., & Dale, B. E. (2005). Understanding factors that limit enzymatic hydrolysis of biomass: Characterization of pretreated corn stover. *Applied Biochemistry and Biotechnology*, *121–124*, 1081–1099. https://doi.org/10.1385/abab:124:1-3:1081

Lawoko, M., Henriksson, G., & Gellerstedt, G. (2005). Structural Differences between the Lignin−Carbohydrate Complexes Present in Wood and in Chemical Pulps. *Biomacromolecules*, *6*(6), 3467–3473. https://doi.org/10.1021/bm058014q

Li, X.-L., Špániková, S., De Vries, R. P., & Biely, P. (2007). Identification of genes encoding microbial glucuronoyl esterases. *FEBS Letters*, *581*(21), 4029–4035. https://doi.org/10.1016/j.febslet.2007.07.041

MacDonald, J., Doering, M., Canam, T., Gong, Y., Guttman, D. S., Campbell, M. M., & Master, E. R. (2011). Transcriptomic Responses of the Softwood-Degrading White-Rot Fungus Phanerochaete carnosa during Growth on Coniferous and Deciduous Wood. *Applied and Environmental Microbiology*, *77*(10), 3211–3218. https://doi.org/10.1128/AEM.02490-10

Mosbech, C., Holck, J., Meyer, A. S., & Agger, J. W. (2018a). The natural catalytic function of CuGE glucuronoyl esterase in hydrolysis of genuine lignin–carbohydrate complexes from birch. *Biotechnology for Biofuels*, *11*(1), 71. https://doi.org/10.1186/s13068-018-1075-2

Mosbech, C., Holck, J., Meyer, A. S., & Agger, J. W. (2018b). The natural catalytic function of CuGE glucuronoyl esterase in hydrolysis of genuine lignin–carbohydrate complexes from birch. *Biotechnology for Biofuels*, *11*(1), 71. https://doi.org/10.1186/s13068-018-1075-2

Nanda, S., Dalai, A. K., & Kozinski, J. A. (2014). Butanol and ethanol production from lignocellulosic feedstock: Biomass pretreatment and bioconversion. *Energy Science & Engineering*, *2*(3), 138–148. https://doi.org/10.1002/ese3.41

Nanda, S., Rana, R., Sarangi, P. K., Dalai, A. K., & Kozinski, J. A. (2018). A Broad Introduction to First-, Second-, and Third-Generation Biofuels. In P. K. Sarangi, S. Nanda, & P. Mohanty (Eds.), *Recent Advancements in Biofuels and Bioenergy Utilization* (pp. 1–25). Springer Singapore. https://doi.org/10.1007/978-981-13-1307-3_1

Okolie, J. A., Nanda, S., Dalai, A. K., & Kozinski, J. A. (2021). Chemistry and Specialty Industrial Applications of Lignocellulosic Biomass. *Waste and Biomass Valorization*, *12*(5), 2145–2169. https://doi.org/10.1007/s12649-020-01123-0

O'Sullivan, A. C. (1997). Cellulose: The structure slowly unravels. *Cellulose*, *4*(3), 173–207. https://doi.org/10.1023/A:1018431705579

Paul, S., & Dutta, A. (2018). Challenges and opportunities of lignocellulosic biomass for anaerobic digestion. *Resources, Conservation and Recycling*, *130*, 164–174. https://doi.org/10.1016/j.resconrec.2017.12.005

Pentari, C., Katsimpouras, C., Haon, M., Berrin, J.-G., Zerva, A., & Topakas, E. (2025). Exploring the synergy between fungal CE15 glucuronoyl esterases and xylanases for

lignocellulose saccharification. *Biotechnology for Biofuels and Bioproducts*, *18*(1), 38. https://doi.org/10.1186/s13068-025-02639-0

Ragauskas, A. J., Williams, C. K., Davison, B. H., Britovsek, G., Cairney, J., Eckert, C. A., Frederick, W. J., Hallett, J. P., Leak, D. J., Liotta, C. L., Mielenz, J. R., Murphy, R., Templer, R., & Tschaplinski, T. (2006). The Path Forward for Biofuels and Biomaterials. *Science*, *311*(5760), 484–489. https://doi.org/10.1126/science.1114736

Raji, O., Arnling Bååth, J., Vuong, T. V., Larsbrink, J., Olsson, L., & Master, E. R. (2021). The coordinated action of glucuronoyl esterase and α-glucuronidase promotes the disassembly of lignin–carbohydrate complexes. *FEBS Letters*, *595*(3), 351–359. https://doi.org/10.1002/1873-3468.14019

Rosso, M.-N., Berrin, J.-G., & Lomascolo, A. (2022). Plant wastes and sustainable refineries: What can we learn from fungi? *Current Opinion in Green and Sustainable Chemistry*, *34*, 100602. https://doi.org/10.1016/j.cogsc.2022.100602

Salas-Veizaga, D. M., Bhattacharya, A., Adlercreutz, P., Stålbrand, H., & Karlsson, E. N. (2021). Glucuronosylated and linear xylooligosaccharides from Quinoa stalks xylan as potential prebiotic source for growth of Bifidobacterium adolescentis and Weissella cibaria. *LWT*, *152*, 112348. https://doi.org/10.1016/j.lwt.2021.112348

Santos, R. B., Hart, P., Jameel, H., & Chang, H. (2013). Wood Based Lignin Reactions Important to the Biorefinery and Pulp and Paper Industries. *BioResources*, *8*(1), 1456–1477. https://doi.org/10.15376/biores.8.1.1456-1477

Sapouna, I., & Lawoko, M. (2021). Deciphering lignin heterogeneity in ball milled softwood: Unravelling the synergy between the supramolecular cell wall structure and molecular events. *Green Chemistry*, *23*(9), 3348–3364. https://doi.org/10.1039/D0GC04319B

Shah, A. A., Seehar, T. H., Sharma, K., & Toor, S. S. (2022). Biomass pretreatment technologies. In *Hydrocarbon Biorefinery* (pp. 203–228). Elsevier. https://doi.org/10.1016/B978-0-12-823306-1.00014-5

Singhvi, M. S., & Gokhale, D. V. (2019). Lignocellulosic biomass: Hurdles and challenges in its valorization. *Applied Microbiology and Biotechnology*, *103*(23–24), 9305–9320. https://doi.org/10.1007/s00253-019-10212-7

Špániková, S., & Biely, P. (2006). Glucuronoyl esterase – Novel carbohydrate esterase produced by *Schizophyllum commune*. *FEBS Letters*, *580*(19), 4597–4601. https://doi.org/10.1016/j.febslet.2006.07.033

Špániková, S., Poláková, M., Joniak, D., Hirsch, J., & Biely, P. (2007). Synthetic esters recognized by glucuronoyl esterase from Schizophyllum commune. *Archives of Microbiology*, *188*(2), 185–189. https://doi.org/10.1007/s00203-007-0241-x

St John, F. J., González, J. M., & Pozharski, E. (2010). Consolidation of glycosyl hydrolase family 30: A dual domain 4/7 hydrolase family consisting of two structurally distinct groups. *FEBS Letters*, *584*(21), 4435–4441. https://doi.org/10.1016/j.febslet.2010.09.051

St. John, F. J., Rice, J. D., & Preston, J. F. (2006). Characterization of XynC from *Bacillus subtilis* subsp. *Subtilis* Strain 168 and Analysis of Its Role in Depolymerization of Glucuronoxylan. *Journal of Bacteriology*, *188*(24), 8617–8626. https://doi.org/10.1128/JB.01283-06

Tarasov, D., Leitch, M., & Fatehi, P. (2018). Lignin–carbohydrate complexes: Properties,

applications, analyses, and methods of extraction: a review. *Biotechnology for Biofuels*, *11*(1), 269. https://doi.org/10.1186/s13068-018-1262-1

Vršanská, M., Kolenová, K., Puchart, V., & Biely, P. (2007). Mode of action of glycoside hydrolase family 5 glucuronoxylan xylanohydrolase from *Erwinia chrysanthemi*. *The FEBS Journal*, *274*(7), 1666–1677. https://doi.org/10.1111/j.1742-4658.2007.05710.x

Wang, S., Dai, G., Yang, H., & Luo, Z. (2017). Lignocellulosic biomass pyrolysis mechanism: A state-of-the-art review. *Progress in Energy and Combustion Science*, *62*, 33–86. https://doi.org/10.1016/j.pecs.2017.05.004

Wegener, G. (2004). Tetsuo Koshijima and Takashi Watanabe: Association between lignin and carbohydrates in wood and other plant tissues. (Springer Series in Wood Science). *Wood Science and Technology*, *37*(5), 451–451. https://doi.org/10.1007/s00226-003-0197-1

Yeoman, C. J., Han, Y., Dodd, D., Schroeder, C. M., Mackie, R. I., & Cann, I. K. O. (2010). Thermostable Enzymes as Biocatalysts in the Biofuel Industry. In *Advances in Applied Microbiology* (Vol. 70, pp. 1–55). Elsevier. https://doi.org/10.1016/S0065-2164(10)70001-0

8 Appendix

Table 8-1. The details of preparing Mcllvaine pH buffer.

pH value	0.2 mol/L Na_2HPO_4	0.1 mol/L Citric Acid
3.2	4.94±1.00	15.06±1.00
4.4	8.82±1.00	11.18±1.00
5.6	11.60±1.00	8.40±1.00
6.0	12.63±1.00	7.37±1.00
6.5	14.00±1.00	6.00±1.00
7.0	16.47±1.00	3.53±1.00
7.5	18.50±1.00	1.50±1.00
8.0	19.45±1.00	0.55±1.00

Figure 8-1. Example of standard curve used in Bradford assay.

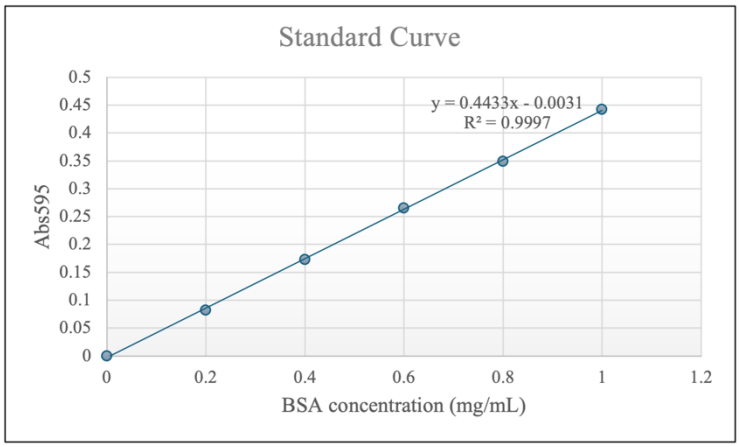

Figure 8-2. Plots of Michaelis Menten equation

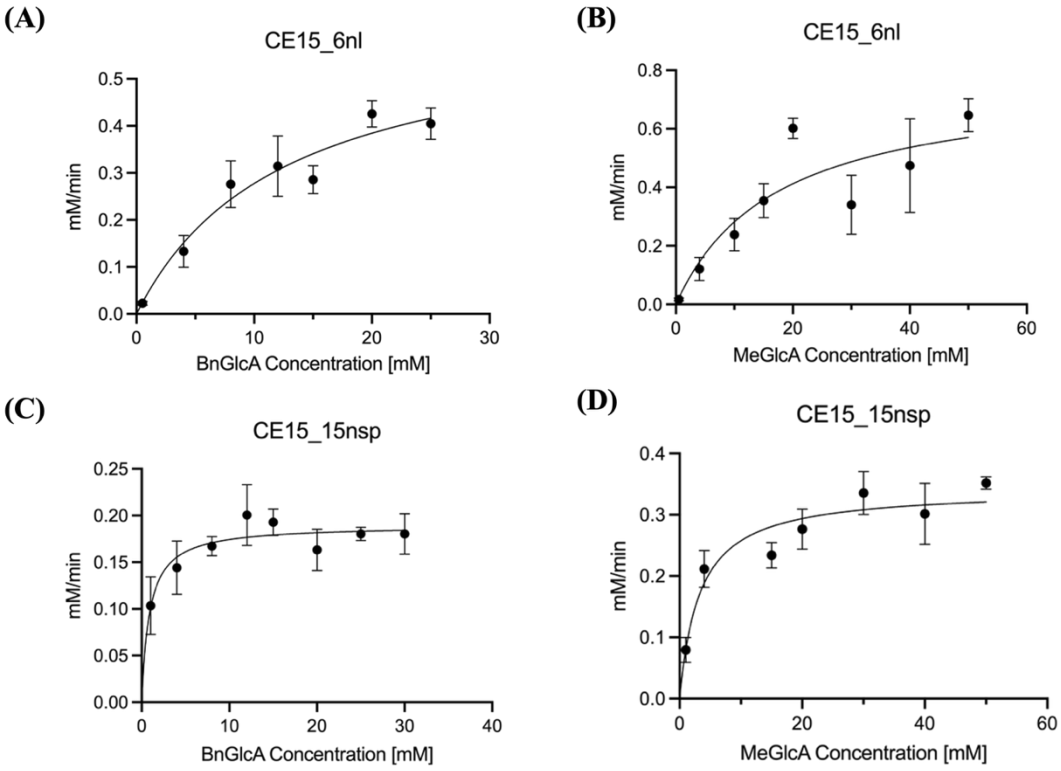

(E)

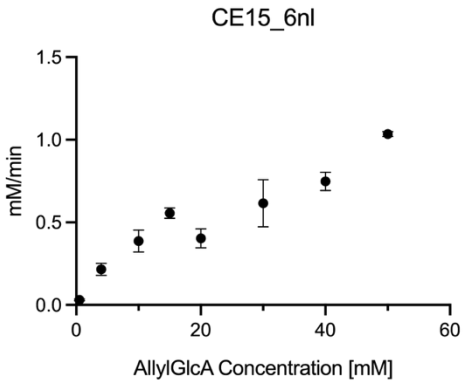
CE15_6nl
mM/min
1.5
1.0
0.5
0.0
0
20
40
60
AllylGlcA Concentration [mM]

(F)

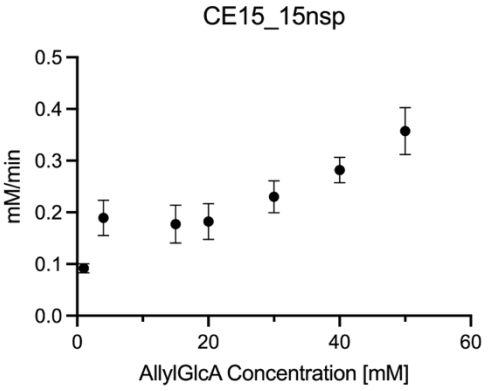
CE15_15nsp
mM/min
0.5
0.4
0.3
0.2
0.1
0.0
0
20
40
60
AllylGlcA Concentration [mM]